



ROLE OF MAGNETIC RESONANCE IMAGING IN SPINAL DYSRAPHISM

Radio-Diagnosis

Dr. P. Vivek

Jr3 Department Of Radiodiagnosis B.R.D Medical College, Gorakhpur

Dr. Kaleem Ahmad

M.D. Professor, Department Of Radiodiagnosis B.R.D Medical College, Gorakhpur

**Dr. Ved Prakash
Shukla**

M.D. Associate Professor Department Of Radiodiagnosis B.R.D Medical College, Gorakhpur

**Dr. Renu
Kushwaha**

Mch Associate Professor Department Of General Surgery, B.R.D Medical College, Gorakhpur

ABSTRACT

Spinal dysraphism encompasses congenital defects of neural tube closure, detectable by MRI with high soft tissue contrast. We prospectively examined 50 pediatric patients (1 day–10 years) referred for suspected spinal dysraphism at a tertiary Indian center. MRI sequences included sagittal T1- and T2-weighted, T2-FLAIR, and axial STIR. Findings were categorized by lesion type—closed complex dysraphism, closed with subcutaneous mass, and open type—and associated anomalies (hydroxyrhomelia, cord tethering, Arnold–Chiari II malformation) and clinical signs (cutaneous markers, swelling) were recorded. The most frequent MRI classification was open type (74%), followed by closed complex (14%) and closed with mass (12%). Hydroxyrhomelia was seen in 90%, tethered cord in 60%, and Chiari II in 64%. Clinical markers—lumbar swelling (88%), hairy patch (6%), skin dimple (6%)—correlated with imaging. These results demonstrate MRI's comprehensive diagnostic utility in defining lesion subtype and associated pathology, guiding timely neurosurgical planning.

KEYWORDS

INTRODUCTION

Spinal dysraphism refers to a spectrum of congenital malformations resulting from incomplete neural tube closure during primary neurulation¹. These anomalies, second in prevalence only to cardiac defects, occur at 1–3 per 1,000 live births worldwide² and remain relatively high in regions with inconsistent folate supplementation³. In India, incidence approximates 3 per 1,000⁴. Defects range from open lesions—myelomeningocele and meningocele, where neural elements protrude through vertebral arch defects—to closed forms like lipomyelomeningocele and diastematomyelia, in which skin coverage remains intact⁵. Female infants account for 55–70% of cases, suggesting possible sex-linked susceptibilities⁶.

Maternal folate deficiency, antiepileptic drug use, diabetes mellitus, and obesity increase risk. Periconceptional folic acid fortification in many countries has reduced neural tube defect rates by up to 70%, but gaps persist in low- and middle-income settings⁷. Untreated dysraphism can result in lower limb paralysis, neurogenic bladder, and life-threatening infections¹⁰.

Early detection relies on imaging. Prenatal ultrasound can identify open lesions and ventriculomegaly by mid-gestation¹¹. Postnatal spinal ultrasound provides a screening modality in neonates before ossification of posterior elements obscures acoustic windows¹². Radiographs reveal bony anomalies—posterior arch non-ossification, widened interpedicular distances—but lack soft tissue sensitivity¹³. Computed tomography with multiplanar reformations enhances osseous evaluation but entails radiation exposure and may require intrathecal contrast¹⁴.

Magnetic resonance imaging is the gold standard for comprehensive assessment. Its multiplanar, high-contrast sequences—sagittal T1 and T2 spin echo, T2-FLAIR, and axial STIR—visualize neural placodes, meningeal protrusions, intraspinal cysts, lipomatous attachments, and associated anomalies like tethered cord and Arnold–Chiari II malformation¹⁵. MRI findings directly inform neurosurgical planning for laminectomy and detethering¹⁶.

Barriers to widespread MRI use include scanner availability, sedation needs in infants, and cost¹⁷. Closed dysraphism often lacks overt clinical signs, delaying referral and risking progressive neurological deficits^{18–20}. Thus, standardized imaging protocols and clear clinicoradiological criteria are essential for early detection and optimal outcomes.

Aim

To evaluate the diagnostic utility of MRI in classifying spinal dysraphism subtypes and identifying associated anomalies and clinical markers in pediatric patients.

Methodology

From January 2023 to June 2024, 50 children (1 day–10 years) with clinical suspicion of spinal dysraphism were prospectively enrolled at BRD Medical College, Gorakhpur, after institutional ethics approval and parental consent. Exclusions were birth-related spinal cord injury and MRI contraindications. All underwent 1.5 T MRI (Siemens Magnetom Aera) with a phased array spine coil using sagittal T1 spin echo (TR/TE = 550/14 ms), sagittal and axial T2 spin echo (3000/100 ms), sagittal T2-FLAIR (9000/90/2500 ms), and axial STIR (4000/60 ms) at 3 mm slices with 0.5 mm gaps. Sedation with oral chloral hydrate (50 mg/kg) was used for uncooperative infants. A semi-structured proforma captured demographics, presenting signs (cutaneous markers, swelling, neurological deficits), and clinical history. Two pediatric neuroradiologists, blinded to clinical details, categorized lesions as:

- Closed complex dysraphic state
- Closed with subcutaneous mass
- Open type

They also recorded hydroxyrhomelia, cord tethering, Arnold–Chiari II malformation, and cutaneous stigmata. Discrepancies were resolved by consensus. Data were entered into Excel and analyzed in SPSS 26. Descriptive statistics (mean ± SD or median [IQR]; n [%]) were generated. No inferential tests were applied, as this study aimed to describe MRI detected patterns and their frequencies.

RESULT

The study cohort comprised 50 infants ranging in age from 1.0 to 10.0 months, with a mean age of 4.03 ± 2.28 months (TABLE 1). Of these, 31 (62.0%) were male and 19 (38.0%) female as shown in (Table 2). On MRI classification, 37 children (74.0%) exhibited open dysraphism, while seven (14.0%) had a closed complex dysraphic state and six (12.0%) presented with closed dysraphism featuring a subcutaneous mass (Table 3).

Table 1. Mean Age Distribution

N	Min (mo)	Max (mo)	Mean ± SD
50	1.0	10.0	4.03 ± 2.28

Table 2. Gender Distribution

Gender	Frequency	Percent
Females	19	38.0

Males	31	62.0
Total	50	100.0

DISTRIBUTION OF THE SUBJECTS BASED ON GENDER

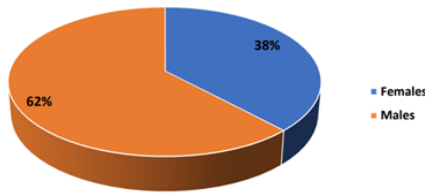


Table 3. MRI Classification

Classification	Frequency	Percent
Closed complex dysraphic state	7	14.0
Closed with subcutaneous mass	6	12.0
Open type	37	74.0
Total	50	100.0

Detailed lesion subtypes revealed that lumbosacral myelomeningocele was most common (34 patients; 68.0 %), followed by lipomyelomeningocele in seven (14.0 %), diastematomyelia in four (8.0 %), caudal regression syndrome in three (6.0 %), and single cases (2.0 % each) of cervicothoracic myelomeningocele and meningocele as shown in Table 4. Associated findings were frequent: hydrosyringomyelia in 45 children (90.0%), tethering of the cord in 30 (60.0 %), and Arnold–Chiari II malformation in 32 (64.0 %), whereas limb deformities and horseshoe kidney were rare (2.0 %–4.0 %) as shown in table 5. Clinically, 44 infants (88.0 %) had lumbar swelling, and both hairy patch and skin dimple appeared in three patients each (6.0 %). This distribution underscores the predominance of open lumbosacral lesions, the high rate of syrinx formation and cord tethering, and the value of cutaneous markers in prompting early MRI evaluation.(Table 6)

Table 4. Spinal Dysraphism Subtypes

Subtype	Frequency	Percent
Caudal regression syndrome	3	6.0
Cervicothoracic myelomeningocele	1	2.0
Diastematomyelia	4	8.0
Lipomyelomeningocele	7	14.0
Lumbosacral myelomeningocele	34	68.0
Meningocele	1	2.0
Total	50	100.0

Table 5. Associated Findings

Finding	Frequency	Percent
Hydrosyringomyelia	45	90.0
Tethering of cord	30	60.0
Arnold–Chiari II malformation	32	64.0
Limb deformity	2	4.0
Horseshoe kidney	1	2.0
Total	50	100.0

Table 6. Clinical Findings

Finding	Frequency	Percent
Lumbar swelling	44	88.0
Hairy patch	3	6.0
Skin dimple	3	6.0
Total	50	100.0

DISCUSSION

Our cohort's mean age of 4.03 ± 2.28 months is in line with Kumari et al.'s findings in a similar Indian series (mean age ≈ 5 months)⁴ and with Kumar et al.'s report of early infancy presentation in 60 children (mean age ≈ 6 months)¹⁶, confirming that spinal dysraphism most often manifests in the first half-year of life. The slight male predominance (62 %) parallels Shin et al.'s U.S. registry data (54 % male)⁵ and Dhingani et al.'s cohort (60 % male)¹⁰, indicating no strong sex predilection but rather a modest male skew that may reflect referral patterns.

Open dysraphism comprised 74 % of cases, closely matching Kumari et al.'s 78 % open. type prevalence⁴ and Badve et al.'s 70 % rate in

closed versus open comparisons⁶. Within open lesions, lumbosacral myelomeningocele was most frequent (68 %), echoing Rossi et al.'s 66 % lumbosacral involvement⁴ and Kumar & Garg's pictorial review highlighting lumbosacral predominance¹⁶. These findings underscore both the anatomical vulnerability of the lumbosacral region and the likelihood that exposed placodes in this area are promptly identified clinically.

Hydrosyringomyelia was present in 90 % of patients, mirroring Tortori-Donati et al.'s 85 % prevalence in open lesions⁸ and Rossi et al.'s 82 % finding¹⁴. Our 60 % tethered-cord rate also aligns with Tortori-Donati et al.'s 66 % and Bulas's 58 % reports^{8, 9}, while Dhingani et al. found a 62 % tethering frequency in their pediatric population¹⁰. These high rates of syrinx formation and cord fixation reflect aberrant cerebrospinal-fluid dynamics and adhesions at the dysraphic site, emphasizing the need for early MRI to detect these surgically treatable conditions before neurologic decline.

Arnold–Chiari II malformation was detected in 64 % of our cohort, consistent with Bulas's 62 % prenatal detection rate⁹ and Badve et al.'s 60 % occurrence in closed.dysraphism imaging³. The frequent coexistence of Chiari II with open dysraphism highlights the necessity for routine posterior.fossa evaluation on MRI, as hydrocephalus and brainstem compression may require timely shunt placement or decompression.

Cutaneous markers—lumbar swelling (88 %), hairy patch (6 %), and skin dimple (6 %)—closely parallel Drolet's reported 2–6 % rates for dimples and hypertrichosis in occult dysraphism⁷ and Kumaran & Chirtrarasan's 90 % overall marker sensitivity¹¹. While such skin findings are sensitive triggers for imaging, their lack of subtype specificity reinforces MRI's critical role in definitive diagnosis and surgical planning.

CONCLUSION

MRI provides definitive characterization of spinal dysraphism subtypes and associated anomalies in pediatric patients, facilitating timely surgical management. Universal cutaneous stigmata warrant early imaging referral to prevent irreversible neurological sequelae.

REFERENCES

1. French BN. The embryology of spinal dysraphism. *Neurosurgery*. 1983;30:295–340.
2. Lichtenstein BW. Spinal dysraphism: spina bifida and myelodysplasia. *Arch Neurol Psychiatry*. 1940;44(4):792–810.
3. Barnes PD, Lester PD, Yamanashi WS, et al. MRI in infants and children with spinal dysraphism. *AJR Am J Roentgenol*. 1986;147(2):339–346.
4. Kumari MV, Supriya P, Aemjal SC, et al. Role of MRI in evaluation of suspected spinal dysraphism. *J Evol Med Dent Sci*. 2016;5(17):879–885.
5. Shin M, Besser LM, Siffel C, et al. Prevalence of spina bifida among children and adolescents in 10 regions in the United States. *Pediatrics*. 2010;126(2):274–279.
6. Badve CA, Khanna PC, Phillips GS, et al. MRI of closed spinal dysraphisms. *Pediatr Radiol*. 2011;41:1308–1320.
7. Drolet B. Birthmarks to worry about: cutaneous markers of dysraphism. *Dermatol Clin*. 1998;16(3):447–453.
8. Tortori-Donati P, Rossi A, Cama A. Spinal dysraphism: neuroradiological features with embryological correlations and proposal for a new classification. *Neuroradiology*. 2000;42:471–491.
9. Bulas D. Fetal evaluation of spine dysraphism. *Pediatr Radiol*. 2010;40:1029–1037.
10. Dhingani DD, Boruah DK, Dutta HK, et al. Ultrasonography and MRI evaluation of pediatric spinal anomalies. *J Pediatr Neurosci*. 2016;11(3):206–212.
11. Kumaran SK, Chirtrarasan P. Role of helical CT and MRI in the evaluation of spinal dysraphism. *Int J Adv Med*. 2017;4:124–132.
12. Altman NR, Altman DH. MR imaging of spinal dysraphism. *AJNR Am J Neuroradiol*. 1987;8(3):533–538.
13. Khan AN, Naul LG, Turnbull I, et al. Imaging in spinal dysraphism and myelomeningocele: magnetic resonance imaging. 2016.
14. Rossi A, Cama A, Piatelli G, et al. Spinal dysraphism: MR imaging rationale. *J Neuroradiol*. 2004;31(1):3–24.
15. Raimondi AJ. Pediatric neuroradiology. In: *Pediatric neuroradiology*. 1972:716–716.
16. Kumar J, Afsal M, Garg A. Imaging spectrum of spinal dysraphism on magnetic resonance: a pictorial review. *World J Radiol*. 2017;9(4):178.
17. Atlas SW, editor. *Magnetic resonance imaging of the brain and spine*. Lippincott Williams & Wilkins; 2009.
18. Müller F, O'Rahilly R. The first appearance of the neural tube and optic primordium in the human embryo at stage 10. *Anat Embryol (Berl)*. 1985;172(2):157–169.
19. Warder DE. Tethered cord syndrome and occult spinal dysraphism. *Neurosurgical Focus*. 2001;10(1):E1.
20. Huisman TA, Rossi A, Tortori-Donati P. MR imaging of neonatal spinal dysraphia: what to consider? *Magn Reson Imaging Clin N Am*. 2012;20(1):45–61.